# Decays of mass-separated $^{138}$Xe and $^{138}$Cs

G. H. Carlson, W. L. Talbert, Jr., and J. R. McConnell
*Ames Laboratory, USAEC and Department of Physics, Iowa State University, Ames, Iowa 50010*
(Received 30 May 1973)

The $\beta$ and subsequent $\gamma$ decays of $^{138}$Xe and $^{138}$Cs were investigated using the on-line isotope separator system TRISTAN at the Ames Laboratory research reactor. Ge(Li) $\gamma$-ray singles and Ge(Li)-Ge(Li) $\gamma$-$\gamma$ coincidence measurements were used to construct level schemes for $^{138}$Cs and $^{138}$Ba. For the decay of $^{138}$Xe, 94 of 99 observed $\gamma$-ray transitions have been placed in a level scheme for $^{138}$Cs with 27 excited states. For the decay of $^{138}$Cs, 82 of 86 observed $\gamma$ rays are placed in a level scheme for $^{138}$Ba with 35 excited states. Ge(Li)-plastic coincidence measurements gave $Q$ values of $2.83 \pm 0.08$ MeV and $5.29 \pm 0.07$ MeV for $^{138}$Xe and $^{138}$Cs, respectively. Spin and parity assignments have been deduced using $\gamma$-ray transition rates, $\beta$-decay log*ft* values, and other information existing in the literature. Interpretation of some of the energy levels is made from a shell-model viewpoint.

## I. INTRODUCTION

This study was undertaken as part of a systematic program to study short-lived gaseous fission product activities. Of particular interest is the nuclear structure near the closed shells $Z = 50$ and $N = 82$. To obtain detailed knowledge of structure in this region, the decays of 14.2-min $^{138}$Xe to 32.2-min $^{138}$Cs and the subsequent decay of $^{138}$Cs to stable $^{138}$Ba were studied. Decay energies of these nuclei were determined from analysis of $\beta$-$\gamma$ coincidence experiments, and level schemes for $^{138}$Cs and $^{138}$Ba, supported by Ge(Li)-Ge(Li) coincidence results, are proposed.

The $^{138}$Ba level scheme has been the object of a great number of experimental and theoretical studies. There are two major reasons why this nucleus has been the object of such a number of studies. First, there are many means for studying the level structure of $^{138}$Ba since it and several of its neighbors are stable. Second, accurate comprehensive information for this nucleus is valuable from a shell-model viewpoint because of its closed neutron configuration. The states in $^{138}$Ba have been studied by inelastic scattering[1-8] and Coulomb excitation[9,10] on stable $^{138}$Ba, deuteron stripping reactions[8,11,12] on stable $^{137}$Ba, the ($^3$He, *d*) and (*d*, $^3$He) reactions[13] on stable $^{138}$Ba, the (*d*, $^3$He) reaction[14] on stable $^{139}$La, and by thermal neutron capture[15,16] by stable $^{137}$Ba. The excited states of $^{138}$Ba are also reached in the $\beta$ decay of $^{138}$Cs produced either directly in fission[17] or as a daughter decay product[18-22] of $^{138}$Xe. The many means for studying this nucleus not only provide complete and accurate knowledge of this level scheme but also provide an excellent opportunity to compare the types of experiments and their results.

Several studies of the decay of $^{138}$Cs have been completed recently while this work was in progress. In most aspects, this work and the most recent other works[17,23-25] agree. However, this work does provide information that was lacking in the other experiments and which led to erroneous interpretations. In the case of a nucleus such as $^{138}$Ba, which has been the object of so much study, such information is valuable and its implications on consistency are needed.

Although the level scheme for $^{138}$Cs does not lend itself to shell-model interpretation as well as does the level scheme for $^{138}$Ba, it is also an important nucleus from a shell-model viewpoint. Excited states of odd-odd nuclei are difficult to interpret, but the structure of $^{138}$Cs might lend itself to shell-model calculations. By studying $N = 82$ nuclei, the proton interactions for $Z > 50$ are explained somewhat successfully by the shell model.[26] The $^{138}$Cs nucleus has only one neutron outside the $N = 82$ closed shell. Reliable calculations have not been performed, but should be plausible in this region.

The $^{138}$Xe decay has been the object of two very recent experimental studies.[27,28] The information presented here does add significant new information to the two recent studies.

## II. EXPERIMENTAL TECHNIQUES

### A. Sample preparation

The TRISTAN on-line isotope separator system described preliminarily in the literature[29,30] and located at the Ames Laboratory research reactor is ideal for studying the so-called inert gases and their daughters that are fission products of $^{235}$U. The source of the fission products is approximately 1 g of uranium in the form of uranyl stearate which is placed in a neutron flux of $3\times10^9$ $n_{th}/cm^2/sec$ at one of the reactor external beams. Of the fission products formed, only the inert gases are free to flow to the ion source of the separator, which is located approximately 2 m from the fission product source. The isotope separator then provides a beam of isotopically pure $^{138}Xe$ which can be deposited on aluminized Mylar tape in a moving tape collector (MTC). The MTC in turn is used to provide isobarically enhanced sources of either the parent $^{138}Xe$ or daughter $^{138}Cs$ activities. The enhancement factors used were approximately 20 to 1 in each case, making unambiguous isobaric identification of the $\gamma$-ray transitions possible. A chemically separated source of $^{138}Cs$ was also used to insure the proper identification of $\gamma$-ray transitions associated with its decay.

### B. Detection methods

Several detectors were used for singles and coincidence experiments. The majority of the counting was done with a pair of 60-$cm^3$-true-coaxial Ge(Li) detectors with efficiencies of 9 and 11% relative to a 7.6-cm by 7.6-cm NaI(Tl) crystal at 1332 keV, with peak height to Compton plateau height of 28.0 and 34.2, and resolution for singles experiments of less than 2.5 keV at 1332 keV. A well-type plastic scintillation detector made of Pilot B plastic with a thickness of 3.5 cm and capable of stopping 6-MeV $\beta$ particles was used for the $\beta$-$\gamma$ coincidence experiments. Low-energy $\gamma$-ray transitions were observed with a 1-$cm^3$-Ge(Li) planar low-energy photon spectrometer and a 300-$mm^2\times$ 3-mm Si(Li) detector.

### C. $\gamma$-ray singles

Singles experiments were performed to determine $\gamma$-ray transition energies and intensities. These experiments consisted of four separate runs; calibration, calibration plus unknown, unknown, and background. The calibration run was used to determine the nonlinearity of the electronics. The nonlinearity information was then used in the calibration plus unknown run to determine energies of intense unknown peaks using the calibration lines as an internal calibration. The newly determined energies were then used to internally calibrate the unknown run and determine the other unknown energies. The background spectrum was useful in identifying contributions to the spectrum from long-lived activities. No evidence was found for any $^{138}I$ activity in the $^{138}Xe$ spectrum studies, and only the most intense transitions from the $A=137$ and $A=139$ decay chains were observed. The energies and intensities for $\gamma$-ray transitions observed in the two decays were determined from standard computer analysis of the singles data and are given in Tables I and II. Typical $\gamma$-ray spectra for $^{138}Xe$ and $^{138}Cs$ decays are shown in Fig. 1. The more intense transitions, and some of the major contaminant peaks (including isobaric contaminants) are labeled in the spectra.

### D. Coincidence techniques

Coincidence techniques for $\gamma$-$\gamma$ and $\beta$-$\gamma$ experiments were similar. Constant fraction timing provided pulse-pair resolution of approximately 30 nsec. The energy analog signals were processed by 4096-channel analog-to-digital converters (ADC's) and the coincidence pairs were stored in a buffer memory capable of holding 2048 pairs of channel addresses. When the memory was filled, its contents were read onto a magnetic tape and the emptied memory was ready to accept data again. The end product was several magnetic tapes, each containing about $3.5\times10^6$ coincidence events in a $4096\times4096$ array. These tapes were played back through a format selection system which made it possible to set a digital gate on a region of interest in one spectrum of the two-parameter array and store counts coincident with this region in the memory of a 16384-channel analyzer. The coincidence information for the two decays was obtained both by visually and by analytically comparing spectra obtained from gates set on $\gamma$-ray peaks and the background region close to the $\gamma$-ray peaks.

For the decay of $^{138}Xe$, coincidence spectra were studied for 32 transitions (and associated background regions); for the decay of $^{138}Cs$, coincidence relations were determined for 20 transitions. In the interest of brevity, the detailed coincidence results are not presented here, but have been tabulated by Carlson.[31] All details of the level schemes presented in this work are consistent with the coincidence information. In the level schemes, positive coincidences are indicated by solid circles and probable coincidences are indicated by open circles.

The experimental techniques of the $\beta$-$\gamma$ coincidence measurements and the methods used in the analysis of these data have been presented in previous papers.[32,33] From analysis of $\beta$ spectra in coincidence with 8 $\gamma$-ray transitions in $^{138}Cs$, the decay energy for $^{138}Xe$ was determined to be $2.83\pm0.08$ MeV, where the error represents an rms deviation for the individual values. For the decay of $^{138}Cs$, a decay energy of $5.29\pm0.07$ MeV was obtained from the analysis of $\beta$ spectra in coincidence with 10 transitions in $^{138}Ba$.

TABLE I. Photopeaks observed in the decay of $^{138}Xe$.

| Energy (keV) | Relative intensity [a] | Placement (keV) | Energy (keV) | Relative intensity [a] | Placement (keV) |
|---|---|---|---|---|---|
| 10.8 [b] | | 10–0 | 912.51 ± 0.07 | 12.2 ± 0.8 | 912–0 |
| 68.3 [c] | | 403–335 | 917.13 ± 0.06 | 33.6 ± 1.8 | 2026–1109 |
| 137.20 ± 0.20 | 2.0 ± 1.0 | 540–403 | 936.36 ± 0.11 | 4.9 ± 0.5 | 951–15 |
| 153.75 ± 0.03 | 169. ± 9. | 412–258 | 941.25 ± 0.08 | 8.2 ± 0.6 | 951–10 |
| 197. [d] | | 1109–912 | 946.63 ± 0.20 | 2.3 ± 0.4 | 1205–258 |
| 242.56 ± 0.05 | 113. ± 6. | 258–15 | 953.1 ± 0.5 | 1.0 ± 0.4 | 2490–1537 |
| 258.31 ± 0.05 | 1000. ± 60. | 258–0 | 996.76 ± 0.30 | 2.3 ± 0.6 | 1537–540 |
| 282.51 ± 0.06 | 14.0 ± 0.9 | 540–258 | 1076.38 ± 0.22 | 3.2 ± 0.6 | 1488–412 |
| 325.3 ± 0.3 | 0.75 ± 0.25 | 335–10 | 1093.87 ± 0.09 | 14.9 ± 0.9 | 1109–15 |
| 329.4 ± 0.5 | 0.50 ± 0.24 | | 1098.77 ± 0.11 | 7.8 ± 0.6 | 1109–10 |
| 335.28 ± 0.09 | 3.5 ± 0.3 | 335–0 | 1102.24 ± 0.17 | 3.9 ± 0.5 | 2262–1160 |
| 371.44 ± 0.05 | 16.1 ± 0.9 | 912–540 | 1114.29 ± 0.10 | 58. ± 6. | 2026–912 |
| 396.43 ± 0.05 | 207. ± 11. | 412–15 | 1141.64 ± 0.09 | 18.8 ± 1.2 | 1157–15 |
| 401.36 ± 0.05 | 70. ± 4. | 412–10 | 1145.44 ± 0.18 | 4.8 ± 0.7 | 1160–15 |
| 403. [d] | | 403–0 | 1153.6 ± 0.5 | 1.1 ± 0.6 | 2262–1109 |
| 434.49 ± 0.05 | 659. ± 36. | 450–15 | 1160.96 ± 0.18 | 3.6 ± 0.5 | 1160–0 |
| 500.22 ± 0.06 | 12.1 ± 0.7 | 912–412 | 1189.54 ± 0.21 | 3.0 ± 0.5 | 1205–15 |
| 530.07 ± 0.07 | 8.5 ± 0.6 | 540–10 | 1194.94 ± 0.20 | 3.2 ± 0.5 | 1205–10 |
| 534.0 ± 0.6 | 0.50 ± 0.20 | 2022–1488 | 1204.5 ± 0.4 | 1.3 ± 0.5 | 1205–0 |
| 537.76 ± 0.13 | 3.9 ± 0.5 | 2026–1488 | 1218.7 ± 0.5 | 1.4 ± 0.6 | |
| 540.8 ± 0.6 | 0.7 ± 0.4 | 540–0 | 1228.3 ± 0.4 | 2.3 ± 0.7 | 2337–1109 |
| 555.95 ± 0.09 | 4.0 ± 0.4 | 555–0 | 1311.07 ± 0.24 | 3.2 ± 0.6 | 2262–951 |
| 568.53 ± 0.06 | 10.7 ± 0.6 | 1109–540 | 1356.6 ± 0.4 | 1.9 ± 0.6 | 1372–15 |
| 579.68 ± 0.14 | 2.6 ± 0.4 | | 1361.9 ± 0.6 | 1.3 ± 0.6 | 1372–10 |
| 586.0 ± 0.4 | 0.64 ± 0.24 | 1559–951 | 1381.4 ± 0.3 | 2.6 ± 0.6 | 1793–412 |
| 588.84 ± 0.08 | 4.2 ± 0.3 | 1793–1205 | 1385.5 ± 0.3 | 2.8 ± 0.6 | 2337–951 |
| 619.7 ± 0.5 | 0.7 ± 0.4 | 1160–540 | 1473.2 ± 0.3 | 2.6 ± 0.5 | 1488–15 |
| 647.2 ± 0.5 | 0.5 ± 0.3 | 1559–912 | 1548.9 ± 0.4 | 2.8 ± 0.7 | 1559–10 |
| 654.08 ± 0.08 | 4.9 ± 0.4 | 912–258 | 1571.84 ± 0.16 | 10.0 ± 1.0 | 2022–450 |
| 675.37 ± 0.15 | 2.5 ± 0.4 | 691–15 | 1578.1 ± 0.5 | 1.9 ± 0.7 | 2490–912 |
| 680.24 ± 0.19 | 1.8 ± 0.4 | 691–10 | 1614.57 ± 0.18 | 9.0 ± 1.0 | 2026–412 |
| 691.5 ± 0.4 | 1.1 ± 0.4 | 691–0 | 1646.5 ± 0.3 | 2.5 ± 0.5 | 2337–691 |
| 693.53 ± 0.16 | 3.0 ± 0.4 | 951–258 | 1768.26 ± 0.13 | 635. ± 33. | 2026–258 |
| 697.6 ± 0.4 | 0.8 ± 0.3 | 1109–412 | 1783.4 ± 0.6 | 1.4 ± 0.6 | 1793–10 |
| 703.58 ± 0.17 | 2.0 ± 0.3 | 2262–1559 | 1799.4 ± 0.6 | 1.3 ± 0.5 | 2490–691 |
| 733.9 ± 0.4 | 1.1 ± 0.3 | | 1812.54 ± 0.18 | 6.9 ± 0.7 | 2262–450 |
| 746. [d] | | 1157–412 | 1850.86 ± 0.13 | 51. ± 3. | 2262–412 |
| 755.0 ± 0.6 | 0.9 ± 0.5 | 1205–450 | 1887.3 ± 0.3 | 2.7 ± 0.5 | 2337–450 |
| 774.21 ± 0.15 | 2.3 ± 0.3 | 1109–335 | 1925.36 ± 0.14 | 21.8 ± 1.2 | 2337–412 |
| 778.10 ± 0.19 | 1.6 ± 0.3 | 2337–1559 | 2004.75 ± 0.14 | 208. ± 11. | 2262–258 |
| 792.9 ± 0.4 | 0.8 ± 0.3 | 1205–412 | 2015.82 ± 0.14 | 466. ± 24. | 2026–10 |
| 799.6 ± 0.6 | 0.5 ± 0.3 | 2337–1537 | 2041.2 ± 0.5 | 1.2 ± 0.4 | 2490–450 |
| 816.06 ± 0.18 | 2.5 ± 0.4 | 1372–555 | 2079.17 ± 0.14 | 56. ± 3. | 2337–258 |
| 848.7 ± 0.3 | 1.6 ± 0.4 | 2337–1488 | 2252.26 ± 0.15 | 87. ± 5. | 2262–10 |
| 851.30 ± 0.17 | 2.4 ± 0.4 | 1109–258 | 2266.8 ± 0.5 | 1.5 ± 0.5 | |
| 865.82 ± 0.07 | 10.2 ± 0.7 | 2026–1160 | 2321.90 ± 0.16 | 25.0 ± 1.4 | 2337–15 |
| 869. [d] | | 1205–335 | 2326.9 ± 0.3 | 2.2 ± 0.4 | 2337–10 |
| 869.35 ± 0.06 | 20.7 ± 1.2 | 2026–1157 | 2475.26 ± 0.16 | 12.4 ± 0.8 | 2490–15 |
| 896.87 ± 0.12 | 4.7 ± 0.5 | 912–15 | 2492.61 ± 0.24 | 2.1 ± 0.3 | 2508–15 |
| 902.3 ± 0.3 | 1.6 ± 0.5 | 1160–258 | 2497.56 ± 0.17 | 6.9 ± 0.5 | 2508–10 |

[a] The relative intensity can be converted to transitions per 100 $\beta$ decays using the factor 0.0294, as calculated from the $^{138}Cs$ decay scheme with the total $\beta$ branching to the 10- and 15-keV levels equal to 19.3% and the ground-state $\beta$ branching equal to 0.

[b] Intensity not given since no intensity measurement was attempted.

[c] Energy taken from Ref. 28.

[d] Intensity not given since $\gamma$ ray was observed only in coincidence data.

## III. LEVEL SCHEME

The level schemes for $^{138}$Cs and $^{138}$Ba, given in Figs. 2 and 3, respectively, were constructed using energy sums and differences, in conjunction with the coincidence data and intensities. To avoid building levels on weakly defined levels, a scoring system involving a confidence index (CI) was used. For a particular level, the CI is given by CI = $N_p + N_d + 2N_c + N_{pc}$. $N_p$ and $N_d$ are, respectively, the number of $\gamma$-ray transitions populating and depopulating the level. $N_c$ and $N_{pc}$ are, respectively, the number of positive coincidences and probable coincidences associated with the level. Although this index is somewhat arbitrary, it gives some measure of the certainty that a particular level

TABLE II. Photopeaks observed in the decay of $^{138}$Cs.

| Energy (keV) | Relative intensity [a] | Placement (keV) |
|---|---|---|
| 112.60±0.13 | 1.15±0.15 | 2203–2090 |
| 138.10±0.06 | 15.4 ±0.9 | 2445–2307 |
| 191.96±0.06 | 5.8 ±0.4 | 2090–1898 |
| 193.89±0.08 | 3.8 ±0.3 | 2639–2445 |
| 212.32±0.08 | 2.03±0.17 | 2415–2203 |
| 227.76±0.06 | 17.2 ±0.9 | 2445–2218 |
| 324.90±0.08 | 3.42±0.24 | 2415–2090 |
| 333.86±0.16 | 1.05±0.18 | 2779–2445 |
| 363.93±0.08 | 3.3 ±0.3 | 2779–2415 |
| 365.29±0.13 | 1.69±0.24 | 2583–2218 |
| 368.7 ±0.4 | 0.26±0.10 | 4012–3643 |
| 408.98±0.06 | 54. ±3. | 2307–1898 |
| 421.59±0.07 | 4.9 ±0.3 | 2639–2218 |
| 462.79±0.07 | 357. ±19. | 1898–1435 |
| 516.74±0.12 | 5.0 ±0.6 | 2415–1898 |
| 546.94±0.07 | 126. ±7. | 2445–1898 |
| 575.7 ±0.4 | 0.25±0.10 | 2991–2415 |
| 596.2 ±0.4 | 0.31±0.12 | 3935–3339 |
| 683.59±0.15 | 1.31±0.17 | 2991–2307 |
| 702.92±0.17 | 1.02±0.16 | 3694–2991 |
| 717.7 ±0.3 | 0.49±0.15 | 3163–2445 |
| 754.5 ±0.4 | 0.42±0.15 | 4012–3257 |
| 766.10±0.12 | 1.78±0.18 | 3647–2880 |
| 773.31±0.10 | 2.85±0.22 | 2991–2218 |
| 782.08±0.09 | 4.2 ±0.3 | 2218–1435 |
| 797.7 ±0.5 | 0.7 ±0.3 | 3437–2639 |
| 802.6 ±0.6 | 0.5 ±0.3 | 3442–2639 |
| 813.0 ±0.3 | 0.74±0.22 | 3694–2880 |
| 842.21±0.16 | 1.01±0.14 | 3694–2851 |
| 855.6 ±0.5 | 0.28±0.11 | 3163–2307 |
| 871.80±0.08 | 63. ±3. | 2307–1435 |
| 880.8 ±0.3 | 1.4 ±0.4 | 2779–1898 |
| 935.03±0.12 | 2.25±0.20 | 3242–2307 |
| 946.0 ±0.5 | 0.39±0.16 | 3163–2218 |
| 953.0 ±0.3 | 0.66±0.18 | 2851–1898 |
| 1009.78±0.08 | 379. ±20. | 2445–1435 |
| 1041.4 ±0.3 | 0.80±0.21 | 3922–2880 |
| 1054.32±0.15 | 2.00±0.24 | 3935–2880 |
| 1147.22±0.09 | 15.9 ±0.9 | 2583–1435 |
| 1199.15±0.24 | 2.2 ±0.4 | 4080–2880 |
| 1203.69±0.13 | 5.1 ±0.5 | 2639–1435 |
| 1264.94±0.16 | 1.77±0.22 | 3163–1898 |
| 1343.59±0.09 | 14.8 ±0.8 | 2779–1435 |
| 1359.1 ±0.5 | 0.63±0.25 | 3257–1898 |
| 1386.39±0.21 | 0.99±0.15 | 3694–2307 |
| 1415.68±0.13 | 4.8 ±0.4 | 2851–1435 |
| 1435.86±0.09 | 1000. ±58. | 1435–0 |
| 1445.04±0.25 | 12.7 ±2.5 | 2880–1435 |
| 1495.63±0.23 | 2.4 ±0.5 | 2931–1435 |
| 1555.31±0.10 | 4.8 ±0.3 | 2991–1435 |
| 1614.09±0.20 | 1.8 ±0.3 | 3049–1435 |
| 1717.1 ±0.3 | 1.4 ±0.3 | 3935–2218 |
| 1727.68±0.18 | 1.50±0.18 | 3163–1435 |
| 1748.7 ±0.5 | 0.9 ±0.4 | 3647–1898 |
| 1778.25±0.23 | 1.9 ±0.3 | 4629–2851 |
| 1806.65±0.18 | 1.25±0.15 | 3242–1435 |
| 1821.7 ±0.3 | 0.61±0.14 | 3257–1435 |
| 1903.2 ±0.4 | 0.63±0.19 | 3339–1435 |
| 1941.0 ±0.3 | 1.08±0.22 | |
| 2023.93±0.20 | 1.63±0.21 | 3922–1898 |
| 2062.34±0.17 | 1.54±0.16 | 4508–2445 |
| 2105.9 ±0.3 | 0.77±0.14 | |
| 2114.3 ±0.7 | 0.29±0.13 | 4012–1898 |
| 2210.7 ±0.4 | 3.0 ±0.9 | 3647–1435 |
| 2218.00±0.10 | 214. ±11. | 2218–0 |
| 2487.1 ±0.6 | 0.33±0.11 | 3922–1435 |
| 2499.4 ±0.3 | 2.5 ±0.7 | 3935–1435 |
| 2510.5 ±0.8 | 0.22±0.10 | |
| 2583.15±0.13 | 3.51±0.22 | 2583–0 |
| 2609.3 ±0.3 | 0.49±0.08 | 4508–1898 |
| 2639.59±0.13 | 108. ±6. | 2639–0 |
| 2731.12±0.15 | 1.79±0.11 | 4629–1898 |
| 2806.57±0.17 | 1.50±0.11 | 4242–1435 |
| 2931.4 ±0.4 | 0.30±0.06 | 2931–0 |
| 3049.9 ±0.3 | 0.48±0.07 | 3049–0 |
| 3072.5 ±0.4 | 0.29±0.06 | 4508–1435 |
| 3180.4 ±0.7 | 0.13±0.04 | |
| 3339.01±0.25 | 2.41±0.15 | 3339–0 |
| 3352.6 ±0.3 | 0.56±0.06 | 3352–0 |
| 3366.98±0.25 | 3.64±0.21 | 3367–0 |
| 3437.5 ±0.6 | 0.18±0.05 | 3437–0 |
| 3442.6 ±0.5 | 0.21±0.05 | 3442–0 |
| 3643.3 ±0.4 | 0.38±0.05 | 3643–0 |
| 3652.5 ±0.8 | 0.09±0.03 | 3652–0 |
| 3935.2 ±0.5 | 0.30±0.05 | 3935–0 |
| 4080.1 ±0.5 | 0.30±0.03 | 4080–0 |

[a] The relative intensity can be converted to transitions per 100 $\beta$ decays using the factor 0.075, as calculated from the $^{138}$Ba decay scheme with no ground-state $\beta$ branching.

exists. The logic behind the scoring system is that one has roughly equivalent confidence in a level determined by three transitions as in a level that is determined by only one $\gamma$-ray transition with solid coincidence information. Each case would have a CI of 3. With several exceptions, levels with a CI of less than 4 are entered with a broken line rather than a solid line. The most notable exception is the 2203-keV level in the $^{138}$Ba level scheme which has a CI of 2 but has been reported also in the work of Carraz, Monnand, and Moussa.[17] The other exceptions involve the high-energy levels in $^{138}$Ba at 3049, 3339, and 3367 keV which have also been seen in the $^{138}$Ba$(p,p')$ reaction by Larson *et al.*[7] and are thus entered as solid lines.

On the basis of comparing transition intensities entering and leaving the excited levels in each decay scheme, $\beta$ branches to these levels in the decays were deduced, and $\log ft$ values calculated. Ground-state $\beta$ branches were assumed to be negligible, since the spin and parity of the $^{138}$Cs ground state has been determined to be $3^-$.[34] In the decay of $^{138}$Xe, the combined $\beta$ branch to the low-lying 10- and 15-keV levels in $^{138}$Cs was determined indirectly by comparing the ground-state $\gamma$-ray intensities from an equilibrium-activity sample of $^{138}$Xe and $^{138}$Cs. The results of the $\beta$ branch determinations and $\log f_0 t$ (and, in some cases, $\log f_1 t$) calculations are shown in Tables III and IV for the two decays. The errors in the $\log ft$ values are determined from the uncertainties in the $\beta$ branching including the ground-state $\beta$ branch, and the uncertainties in $T_{1/2}$ and $Q_\beta$. The uncertainties in $\beta$ branching include the effects of possible errors in the choice of $\gamma$-ray multipolarities as well as the uncertainties in the $\gamma$-ray intensities. The level energies and uncertainties given in Tables III and IV were determined from a method which utilized the $\gamma$-ray uncertainties and the other level energy uncertainties to determine weighted averages and, by iteration, determined the minimum sum of all the level uncertainties. The level uncertainties listed are the larger of either the rms errors in $\gamma$-ray placement or the errors propagated through $\gamma$-ray uncertainties and other level uncertainties.

### A. Comparison with other $^{138}$Xe decay studies

A comparison between the level scheme developed in this work (shown in Fig. 2) and the two most recent studies[27,28] of the decay of $^{138}$Xe appears in Table III. In this table, several levels are listed which are reported both in this work and in one of the comparative studies. In most of these cases, this work provided definitive confirmation in terms of coincidence information and close energy-sum relations.

The 335.4- and 403.6-keV levels have not been previously reported. Transitions supporting the

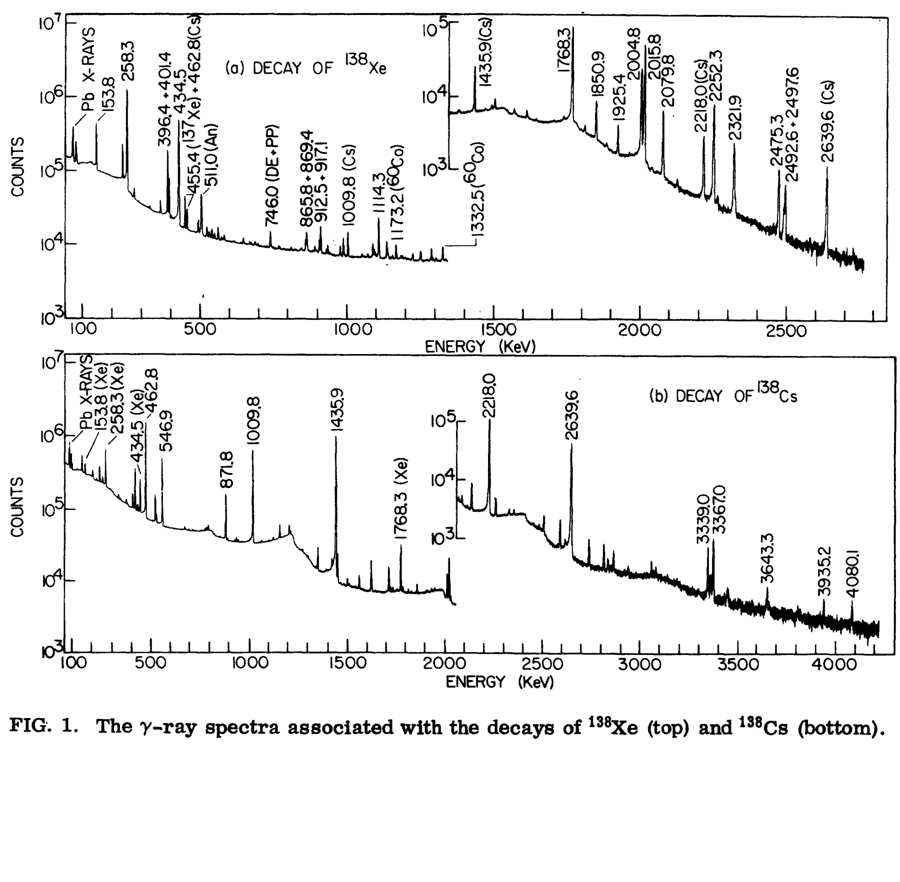


FIG. 1. The $\gamma$-ray spectra associated with the decays of $^{138}$Xe (top) and $^{138}$Cs (bottom).

existence of these levels were subject to interference from intense $\gamma$ rays, a $^{138}$Cs decay transition, and the tail of a Pb x-ray peak. The $\gamma$ ray which was hidden by the x ray was not observed in this experiment but was reported at 68.3 keV by Monnand *et al.*[28] Coincidences of the 137-, 335-, and 403-keV $\gamma$ rays with the 371- and 568-keV $\gamma$ rays feeding the 540.8-keV level indicate that the former transitions should be placed below the 540.8-keV level. Both the 335- and 403-keV tran-

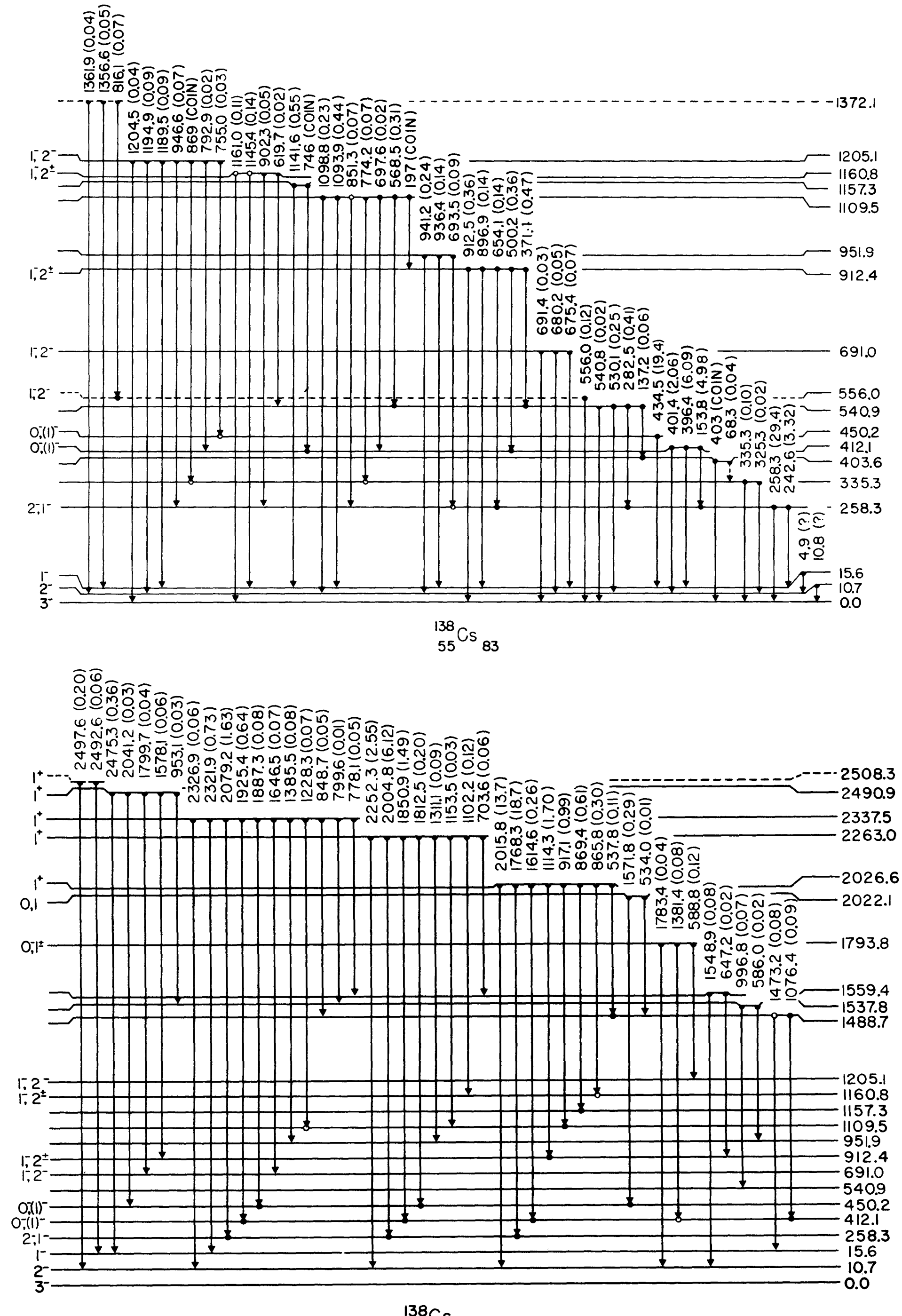


FIG. 2. The level scheme of $^{138}$Cs with $J^{\pi}$ assignments.

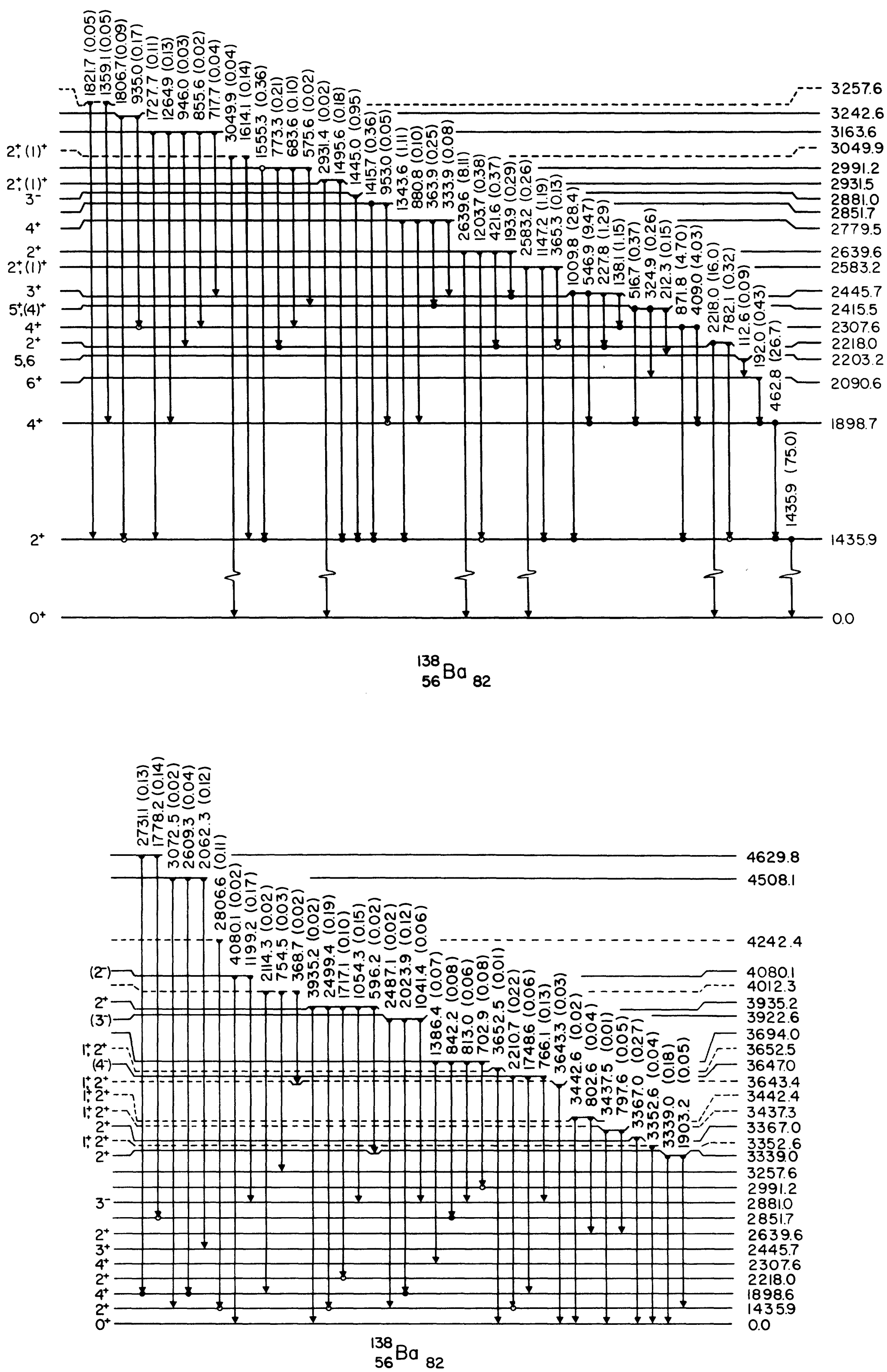

FIG. 3. The level scheme of $^{138}$Ba with $J^{\pi}$ assignments.

sitions were also found to be in coincidence with the 137-keV $\gamma$ ray. The energy sums of the 403- plus 137-keV transitions and 335- plus 137- plus 68-keV transitions are close to 540 keV suggesting cascades with the 137-keV $\gamma$ ray feeding or being fed by the 335-68-keV cascade or the 403-keV $\gamma$ ray. The ordering of the levels is based upon possible coincidences seen in the 335-keV gate at 774 and 869 keV, the latter coincidence also suggesting the presence of a doublet at 869 keV.

In prior works, a discrepancy existed concerning the placement of the 434-keV $\gamma$ ray as feeding either the 10.7-keV level[28] or the 15.7-keV level.[27] Coincidences observed in this study between the 434-keV $\gamma$ ray and the 1812- and 1887-keV $\gamma$ rays from well-established levels suggest strongly that the 434-keV $\gamma$ ray feeds the 15.7-keV level

TABLE III. Comparison of level energies reported in three most recent $^{138}$Xe decay studies, and the corresponding percent $\beta$ branches and log*ft* values from this study.

| Achterberg *et al.* (Ref. 27) level (keV) | Monnand *et al.* (Ref. 28) level (keV) | This work Level (keV) | This work Percent $\beta$ branching | log*ft* [a] (log$f_1t$) [b] |
|---|---|---|---|---|
| 0.0 | 0.0 | 0.0 | ~0.0 | |
| 10.8 | 10.85 | 10.70 ± 0.12 | <22.3 | >6.9 |
| 15.7 | 15.70 | 15.64 ± 0.08 | <22.3 | >6.9 |
| 258.5 | 258.3 | 258.31 ± 0.06 | <4.4 | >7.4 |
| | | 335.31 ± 0.16 | <0.16 | >8.8 |
| | | 403.63 ± 0.20 | <0.35 | >8.4 |
| 412.5 | 412.2 | 412.09 ± 0.06 | 11.5 ± 0.5 | 6.92 ± 0.07 |
| | | | | (8.14) |
| | 445.3 | | | |
| 450.3 | | 450.18 ± 0.13 | 18.4 ± 1.0 | 6.69 ± 0.07 |
| | | | | (7.89) |
| 541.1 | 540.8 | 540.88 ± 0.07 | ~0.0 | |
| | | 555.96 ± 0.08 | 0.04 ± 0.02 | 9.2 ± 0.2 |
| | 691.1 | 691.04 ± 0.16 | 0.05 ± 0.03 | 9.1 ± 0.3 |
| 815.7 | | | | |
| 876.2 | | | | |
| | 881.4 | | | |
| 912.6 | 912.5 | 912.39 ± 0.10 | ~0.0 | |
| 951.6 | 951.9 | 951.93 ± 0.08 | 0.27 ± 0.03 | 8.11 ± 0.10 |
| 1109.7 | 1109.4 | 1109.47 ± 0.06 | <0.12 | >8.3 |
| 1127.0 | | | | |
| | 1157.2 | 1157.26 ± 0.06 | ~0.0 | |
| | | 1160.82 ± 0.12 | ~0.0 | |
| | | 1205.1 ± 0.3 | 0.20 ± 0.03 | 7.99 ± 0.12 |
| | | | | (8.89) |
| 1367.5 | | | | |
| | | 1372.11 ± 0.17 | 0.16 ± 0.03 | 7.92 ± 0.12 |
| | | | | (8.74) |
| 1395.8 | | | | |
| 1489.0 | | 1488.74 ± 0.18 | <0.02 | >8.7 |
| | | 1537.77 ± 0.21 | 0.04 ± 0.02 | 8.3 ± 0.3 |
| | | 1559.45 ± 0.16 | 0.04 ± 0.02 | 8.3 ± 0.3 |
| | | 1793.76 ± 0.24 | 0.23 ± 0.02 | 7.19 ± 0.14 |
| | | | | (7.76) |
| | | 2022.09 ± 0.22 | 0.29 ± 0.03 | 6.7 ± 0.2 |
| | | | | (7.1) |
| 2026.7 | 2026.5 | 2026.61 ± 0.04 | 34.1 ± 1.1 | 4.6 ± 0.2 |
| 2263.0 | 2263.0 | 2262.98 ± 0.10 | 10.0 ± 0.3 | 4.6 ± 0.2 |
| 2337.6 | 2337.5 | 2337.49 ± 0.08 | 3.22 ± 0.10 | 4.9 ± 0.2 |
| 2468.5 | | | | |
| | 2491.0 | 2490.88 ± 0.22 | 0.49 ± 0.03 | 5.2 ± 0.3 |
| 2509.0 | | 2508.26 ± 0.16 | 0.25 ± 0.02 | 5.4 ± 0.4 |

[a] Errors in log*ft* values do not reflect the possibility of a misplaced $\gamma$ ray.

[b] Convention used in Refs. 35 and 36.

rather than the 10.7-keV level, thus establishing the level at 450.2 keV.

Achterberg *et al.*[27] report a level at 815.7 keV which is depopulated by the 556- and 816-keV $\gamma$ rays. The coincidence results show that these $\gamma$ rays are in coincidence with each other, but with no other transitions. They have thus been treated as a cascade to the ground state, giving a level at 1372.2 keV. Achterberg *et al.* report a level at 1367.5 keV using double placement of the 917-keV $\gamma$ ray along with a 1358-keV $\gamma$ ray which has a large energy error. This 1358-keV $\gamma$ ray in their spectrum is probably the unresolved 1356-, 1361-keV doublet, which also depopulates the 1372.2-keV level. The ordering of the 815- and 556-keV $\gamma$-ray cascade was chosen to satisfy the intensity balance at the intermediate level, resulting in a level at 556.0 keV. Since the 1372.2-keV level has a CI of 3 and is thus dotted, the level at 556.0 keV is also dotted, even though it has a larger CI.

The 876.2-keV level reported by Achterberg *et al.* and the 881.4-keV level reported by Monnand *et al.*[28] both depend on the placement of the 865-keV $\gamma$ ray as a depopulating transition. $\gamma$-$\gamma$ coincidence measurements indicate that neither of these possibilities is reasonable but that instead the 865-keV transition feeds the well-established level at 1160.7 keV.

Achterberg *et al.* also report levels at 1127.0, 1395.8, and 2468.5 keV. The level at 1127.0 keV is based on the 869- plus 258-keV and 586- plus 540-keV sums. Coincidence information shows that the 869-keV $\gamma$ ray is not in coincidence with the 258-keV $\gamma$ ray but is a member of the 869-1147-keV cascade depopulating the 2026.6-keV level. The level at 1395.8 keV is reported to be depopulated by the 579-keV $\gamma$ ray to a level at 815.7 keV and the 1384-keV $\gamma$ ray to that at 10.7 keV, and fed by the doubly placed 941-keV $\gamma$ ray. As mentioned, the 815.7-keV level is not consistent with the coincidence results of this work, leaving the basis for a level at 1395.8 keV very weak. The 2468.5-keV level is based on three transitions at 1101, 1358, and 2457 keV. The 2457-keV $\gamma$ ray was not observed in this study; the reported 1358-keV $\gamma$ ray is probably the doublet mentioned in connection with the 1372.2-keV level, and the 1101-keV $\gamma$ ray is reported to feed the level at 1367.5 keV which has been questioned above.

Five other levels were observed in this study that had not been observed before. Three of these levels, at 1537.8, 1559.5, and 2022.6 keV, have CI's of only 4. The 1793.9-keV level is better substantiated with a CI of 5 and the level at 1205.2 keV has a strong CI of 8.

### B. Comparison with other $^{138}$Cs decay studies

A comparison between the level scheme developed in this work (shown in Fig. 3) and the two most recent studies[17,24] of the decay of $^{138}$Cs is contained in Table IV. Five of the levels listed under this work had CI's of only 3 and are entered with dotted lines; these are the 3257.6-, 3352.6-, 3437.4-, 3652.5-, and 4012.3-keV levels. The 3242.5-keV level is better defined with a CI of 4, and the 3694.0-keV level appears to be firm with a CI of 7. Several levels listed in Table IV are reported both in this work and in one of the comparative studies. In these cases, this work provides definitive confirmation in terms of coincidence information and close energy-sum relations.

The placement of the 1415-keV transition in this work leads to a major departure from previous studies. Coincidence data from this work show that the 1415-keV transition is in coincidence with the 1435-keV transition but not in coincidence with the 1009-keV transition as previously supposed, thus defining a level at 2851.6 keV rather than at 3861 keV as reported earlier.[17,23,24] This was a difficult measurement since the 1415-keV $\gamma$-ray peak is on the shoulder of the intense 1435-keV $\gamma$-ray peak which is itself in coincidence with the 1009-keV $\gamma$ ray. There is also one other positive coincidence and two probable coincidences associated with the 2851.6-keV level yielding a strong CI of 10. A $5^-$ level has been seen by Morrison *et al.*[8] at 3860 keV but as this would require a second forbidden $\beta$ transition to be populated directly, it is unlikely to be observed in $\beta$ decay.

The level at 3560.8 keV reported by Carraz, Monnand, and Moussa[17] is not substantiated in this work. The 1343-keV $\gamma$ ray, which was the only transition from this conjectured level, was found to be in coincidence with the 1435-keV $\gamma$ ray and is a major deexcitation of the 2779.4-keV level.

The placement of the 2731-keV $\gamma$ ray causes the discrepancy between the 4629.8-keV level seen in this work and the 4166-keV level reported in previous studies.[17,23,24] The other works have the 2731-keV transition feeding the 1435-keV level from the 4166-keV level, but our coincidence data show that the 462-keV $\gamma$ ray is also in coincidence with the 2731-keV $\gamma$ ray, yielding a level at 4629.8 keV. Except for the 1778-keV $\gamma$ ray, the transitions depopulating the 3880- and 4358-keV levels reported by Hill and Fuller[24] were not observed in this study. The 1778-keV $\gamma$ ray appears to depopulate the 4629-keV level from the observation that it is in possible coincidence with the 1415-keV $\gamma$ ray.

TABLE IV. Comparison of level energies reported in the three most recent decay studies, and the corresponding percent $\beta$ branches and log$ft$ values from this study.

| Hill and Fuller (Ref. 24) level (keV) | Carraz, Monnand, and Moussa (Ref. 17) level (keV) | This work Level (keV) | This work Percent $\beta$ branching | log$ft$ [a] (log$f_1t$) [b] |
|---|---|---|---|---|
| 0.0 | 0.0 | 0.0 | ~0.0 | |
| 1435.7 | 1436.0 | 1435.89 ± 0.05 | 9. ± 5. | 8.25 ± 0.24 |
| 1898.4 | 1899.0 | 1898.68 ± 0.06 | 11.8 ± 1.7 | 7.89 ± 0.07 |
| 2090.1 | 2090.7 | 2090.62 ± 0.06 | 0.11 ± 0.06 | 9.8 ± 0.3 |
| | 2203.2 | 2203.20 ± 0.08 | <0.04 | >10.2 |
| 2217.9 | 2217.8 | 2217.95 ± 0.05 | 14.1 ± 1.1 | 7.63 ± 0.04 |
| 2307.4 | 2307.8 | 2307.64 ± 0.05 | 6.7 ± 0.5 | 7.90 ± 0.04 |
| 2414.9 | 2415.2 | 2415.51 ± 0.05 | 0.54 ± 0.06 | 8.93 ± 0.05 |
| 2445.4 | 2445.8 | 2445.69 ± 0.05 | 40.6 ± 2.4 | 7.03 ± 0.04 (8.37) |
| 2582.8 | 2583.0 | 2583.15 ± 0.07 | 1.59 ± 0.10 | 8.35 ± 0.04 |
| 2639.3 | 2639.3 | 2639.57 ± 0.05 | 9.1 ± 0.6 | 7.55 ± 0.04 (8.84) |
| 2779.2 | | 2779.47 ± 0.06 | 1.54 ± 0.10 | 8.23 ± 0.04 |
| | | 2851.64 ± 0.10 | 0.19 ± 0.04 | 9.09 ± 0.10 |
| 2880.5 | 2881.2 | 2880.94 ± 0.11 | 0.38 ± 0.19 | 8.76 ± 0.22 |
| 2931.1 | | 2931.48 ± 0.20 | 0.20 ± 0.04 | 9.00 ± 0.09 |
| 2990.8 | | 2991.21 ± 0.07 | 0.61 ± 0.04 | 8.47 ± 0.04 |
| 3049.9 | | 3049.94 ± 0.17 | 0.172 ± 0.024 | 8.98 ± 0.07 |
| 3163.5 | | 3163.57 ± 0.14 | 0.33 ± 0.03 | 8.60 ± 0.05 |
| | | 3242.62 ± 0.11 | 0.263 ± 0.022 | 8.64 ± 0.05 |
| | | 3257.64 ± 0.25 | 0.061 ± 0.024 | 9.26 ± 0.18 |
| 3339.5 | 3339.6 | 3339.02 ± 0.19 | 0.204 ± 0.022 | 8.66 ± 0.06 |
| 3352.2 | | 3352.6 ± 0.3 | 0.042 ± 0.005 | 9.34 ± 0.06 |
| 3365.9 | 3367.5 | 3366.98 ± 0.25 | 0.273 ± 0.020 | 8.51 ± 0.05 |
| | | 3437.3 ± 0.4 | 0.063 ± 0.022 | 9.08 ± 0.16 |
| 3442.1 | | 3442.4 ± 0.4 | 0.055 ± 0.023 | 9.14 ± 0.19 |
| | 3560.8 | | | |
| 3641.6 | 3644 | 3643.4 ± 0.3 | <0.02 | > 9.4 |
| 3646.7 | | 3647.01 ± 0.19 | 0.42 ± 0.08 | 8.05 ± 0.09 |
| | | 3652.5 ± 0.8 | 0.007 ± 0.003 | 9.84 ± 0.15 |
| | | 3694.00 ± 0.12 | 0.28 ± 0.03 | 8.18 ± 0.06 |
| 3861.1 | 3860 | | | |
| 3880.0 | | | | |
| 3922.0 | | 3922.58 ± 0.17 | 0.21 ± 0.03 | 8.05 ± 0.07 |
| 3935.4 | | 3935.24 ± 0.13 | 0.49 ± 0.06 | 7.67 ± 0.07 (8.43) |
| | | 4012.3 ± 0.3 | 0.073 ± 0.017 | 8.39 ± 0.11 |
| 4081.0 | | 4080.08 ± 0.23 | 0.19 ± 0.03 | 7.89 ± 0.09 (8.57) |
| 4166.8 | 4166 | | | |
| 4242.3 | 4242 | 4242.45 ± 0.18 | 0.112 ± 0.010 | 7.88 ± 0.07 (8.45) |
| 4357.7 | | | | |
| 4507.4 | | 4508.06 ± 0.14 | 0.174 ± 0.016 | 7.23 ± 0.08 (7.59) |
| | | 4629.83 ± 0.14 | 0.28 ± 0.03 | 6.76 ± 0.09 (7.00) |

[a] Errors in log$ft$ values do not reflect the possibility of a misplaced $\gamma$ ray.
[b] Convention used in Refs. 35 and 36.

TABLE V. Summary of $J^{\pi}$ assignments for levels in $^{138}$Cs populated in $^{138}$Xe decay.

| Level (keV) | $J^{\pi}$ | Reasons |
|---|---|---|
| 0 | $3^-$ | $J=3$ from atomic beam experiment (Ref. 34); negative parity from systematics, shell model; no apparent allowed $\beta$ transitions to levels in $^{138}$Ba; absence of ground-state $\gamma$-ray transitions from $1^+$ levels above 2 MeV. |
| 10.7 | $2^-$ | 10-keV transition is $M1$ (Refs. 27,28); strong $\gamma$-ray transitions from $1^+$ levels at 2026 and 2263 keV exclude $3^-$ or $4^-$; comparison in systematics with $^{140}$La. |
| 15.6 | $1^-$ | 5-keV transition is $M1$ (Ref. 28) ICC measurements (Refs. 27, 28) for transitions linking the 0-, 15-, and 258-keV levels and for transitions linking the 10-, 15-, and 412-keV levels indicate that the 15-keV level has negative parity. Spin of 2 or 3 is unlikely from systematics, shell model, or comparison with neighboring nuclei. |
| 258.3 | $2^-, 1^-$ | ICC measurements (Refs. 27,28) indicate negative parity; transitions linking the 258-keV level with $1^-$, $3^-$, and $1^+$ levels indicates $J^{\pi}$ of $1^-$ or $2^-$. Shell-model description most consistent with assignment of $2^-$ as mentioned in Discussion. |
| 335.3 | $1^-, 2^{\pm}, 3^{\pm}, 4^-$ | Transitions to $3^-$ ground state and $2^-$ first excited state. |
| 403.6 | | No assignment suggested due to lack of definitive singles transition information. |
| 412.1 | $0^-, (1)^-$ | ICC measurements (Refs. 27, 28) indicate negative parity; $\log f_1t=8.1$; no ground-state transition favors $0^-$. |
| 450.2 | $0^-, (1)^-$ | Same reasoning as for 412-keV level; $\log f_1t=7.9$. |
| 540.9 | $1^-, 2^{\pm}, 3^{\pm}, 4^-$ | Same reasoning as for 335-keV level. |
| 556.0 | $1^-, 2^-$ | $\log ft=9.2$ plus transition to $3^-$ level. |
| 691.0 | $1^-, 2^-$ | Same reasoning as for 556-keV level; $\log ft=9.1$. |
| 912.4 | $1^-, 2^{\pm}$ | Transitions to $1^-$ and $3^-$ levels, and from $1^+$ level. |
| 951.9 | $0^-, 1^+, (1^-, 2^-)$ | Transition to $2^-$ 10-keV level; $\log ft=8.1$, no ground-state transition favors $0^-$, $1^+$. |
| 1109.5 | $0^-, 1^+, (1^-, 2^-)$ | Transitions to $1^-$ and $2^-$ levels, and from $1^+$ level; $\log ft=8.3$; no ground-state transition favors $0^-$, $1^+$. |
| 1157.3 | $0^{\pm}, 1^+, (1^-, 2^{\pm})$ | Transition to $1^-$ level and from $1^+$ level; no ground-state transition favors $0^{\pm}$, $1^+$. |
| 1160.8 | $1^-, 2^{\pm}$ | Transitions to $1^-$ and $3^-$ levels, and from $1^+$ level. |
| 1205.1 | $1^-, 2^-$ | Transition to $3^-$ level; $\log ft=8.0$. |
| 1372.1 | $0^-, 1^+, (1^-, 2^-)$ | $\log ft=7.9$; no ground-state transition favors $0^-$, $1^+$. |
| 1488.7 | $0^{\pm}, 1^{\pm}, 2^{\pm}$ | Transition to $1^-$ level and from $1^+$ level. |
| 1537.8 | $0^{\pm}, 1^{\pm}, 2^-$ | $\log ft=8.3$, transition from $1^+$ level. |
| 1559.4 | $0^-, 1^{\pm}, 2^-$ | Transition to $2^-$ level and from $1^+$ level; $\log ft=8.3$. |
| 1793.8 | $0^-, 1^{\pm}$ | Transition to $2^-$ level; $\log f_1t=7.8$. |
| 2022.1 | $0^{\pm}, 1^{\pm}$ | $\log f_1t=7.1$. |
| 2026.6 | $1^+$ | $\log ft=4.6$. |
| 2263.0 | $1^+$ | $\log ft=4.6$. |
| 2337.5 | $1^+$ | $\log ft=4.9$. |
| 2490.9 | $1^+$ | $\log ft=5.2$ |
| 2508.3 | $1^+$ | $\log ft=5.4$ |

TABLE VI. Summary of $J^{\pi}$ assignments for levels in $^{138}$Ba populated in $^{138}$Cs decay.

| Level (keV) | $J^{\pi}$ | Reasons |
|---|---|---|
| 0 | $0^+$ | Ground state for even-even nucleus. |
| 1435.9 | $2^+$ | Coulomb excitation (Refs. 9, 10). |
| 1898.7 | $4^+$ | Transition from $3^+$ 2445-keV level is $M1$ (Ref. 25); proton momentum transfer in $^{139}$La($d$,$^3$He)$^{138}$Ba reaction (Ref. 14) indicates $4^+$ or $6^+$; momentum transfer in inelastic $^4$He scattering (Ref. 6). |
| 2090.6 | $6^+$ | $T_{1/2}=0.8$ nsec (Ref. 17) similar to 2108-keV isomeric state in $^{140}$Ce; populated strongly in the decay of the $6^-$ isomeric state of $^{138}$Cs (Ref. 17); little, if any, $\beta$ branching from the decay of the $3^-$ ground state. |
| 2203.2 | $5^{\pm}, 6^{\pm}, (4^+)$ | Transition to $6^+$, 2090-keV level; no $\beta$ branch from $^{138}$Cs$^g$; $\beta$ branch from $^{138}$Cs$^m$ (Ref. 17). |
| 2218.0 | $2^+$ | Intense ground-state transition, strong $\beta$ branch favor $J=2$; ICC measurements (Ref. 25) and momentum transfer for $(p,p')$ (Ref. 7) and $(\alpha,\alpha')$ (Ref. 6) reactions indicate $2^+$. |
| 2307.6 | $4^+$ | ICC measurements (Ref. 25) plus $\log ft=7.9$, limit $J^{\pi}$ to $3^+$ or $4^+$; $(p,p')$ momentum transfer (Ref. 7) indicates proper choice is $4^+$. |
| 2415.5 | $5^+, (4)^+$ | Transitions to $4^+$ 1898-keV and $6^+$ 2090-keV levels, plus $\log ft=8.9$, limit $J^{\pi}$ to $4^+$ or $5^+$; $\log ft=7.0$ for $\beta$ branch from $^{138}$Cs$^m$ (Ref. 7) indicates a preference for $5^+$. |
| 2445.7 | $3^+$ | ICC (Ref. 25) and angular correlation (Ref. 19) measurements; $\log f_1t=8.4$ and absence of ground-state transition consistent with this assignment. |
| 2583.2 | $2^+, (1)^+$ | Transition to ground state and $\log ft=8.4$ indicate $J^{\pi}$ of $1^+$ or $2^+$; relative strengths of transitions to ground state and 1435-keV level give preference to spin of 2. |
| 2639.6 | $2^+$ | Transition to ground state and $\log ft=7.6$ indicate $J^{\pi}$ of $1^+$ or $2^+$; momentum transfer in $(p,p')$ study (Ref. 7) indicates $2^+$ is the proper choice. |
| 2779.5 | $4^+$ | Transitions to $2^+$ 1435-keV and $4^+$ 1898-keV levels along with $\log ft=8.2$ restrict $J^{\pi}$ to $2^+$, $3^{\pm}$, or $4^+$; momentum transfer in $(p,p')$ study (Ref. 7) indicates $4^+$ is the proper choice. |
| 2851.6 | $3^{\pm}, 4^+, (2^+)$ | Transitions to $2^+$ 1435-keV and $4^+$ 1898-keV levels along with $\log ft=9.1$ restrict $J^{\pi}$ to $2^+, 3^{\pm}$, or $4^+$; lack of ground-state transition favors spin of 3 or 4. |
| 2880.9 | $3^-$ | Transition to $2^+$ 1435-keV level plus $\log ft=8.8$ give range in $J^{\pi}$ of $1^+, 2^{\pm}, 3^{\pm}$, $4^+$; strong presence in $(d,d')$ (Ref. 1) and $(\alpha,\alpha')$ (Ref. 4, 6) studies, with momentum transfer (Ref. 6) strong evidence for $J^{\pi}=3^-$. |
| 2931.5 | $2^+, (1)^+$ | Same reasoning as for 2583-keV level, with $\log ft=9.0$. |
| 2991.2 | $3^{\pm}, 4^+, (2^+)$ | Similar to 2851-keV level, with $\log ft=8.5$ and transitions to $2^+$ 1435-keV and $4^+$ 2307-keV levels. |
| 3049.9 | $2^+, (1)^+$ | Similar reasoning to 2583-keV level, with $\log ft=9.0$. |
| 3163.6 | $3^{\pm}, 4^+, (2^+)$ | Similar reasoning to 2851-keV level, with $\log ft=8.6$. |
| 3242.6 | $3^{\pm}, 4^+, (2^+)$ | Similar reasoning to 2991-keV level, with $\log ft=8.6$. |

TABLE VI *(Continued)*

| Level (keV) | $J^{\pi}$ | Reasons |
|---|---|---|
| 3257.6 | $3^{\pm}, 4^{+}, (2^{+})$ | Similar reasoning to 2851-keV level, with $\log ft = 9.3$. |
| 3339.0 | $2^{+}$ | Transition to ground state plus $\log ft = 8.7$ limit $J^{\pi}$ to $1^{+}$ or $2^{+}$; momentum transfer in $(p,p')$ study (Ref. 7) indicates $J^{\pi} = 2^{+}$ is correct choice. |
| 3352.6 | $1^{+}, 2^{+}$ | Transition to ground state plus $\log ft = 9.3$. |
| 3367.0 | $2^{+}$ | Same reasoning as for 3339-keV level, with $\log ft = 8.5$. |
| 3437.3 | $1^{+}, 2^{+}$ | Same reasoning as for 3352-keV level, with $\log ft = 9.1$. |
| 3442.4 | $1^{+}, 2^{+}$ | Same reasoning as for 3352-keV level, with $\log ft = 9.1$. |
| 3643.4 | $1^{\pm}, 2^{+}$ | Transition to the ground state. |
| 3647.0 | $(4^{-})$ | Possibly the neutron particle-hole state (Ref. 8) of $4^{-}$; consistent with relatively strong $\gamma$ transition to $3^{-}$ 2880-keV level although branching ratio to first and second excited states is inconsistent with this $J^{\pi}$ assignment; $\log ft = 8.1$ indicates a hindered allowed $\beta$ branch. |
| 3652.5 | $1^{+}, 2^{+}$ | Same reasoning as for 3352-keV level, with $\log ft = 9.8$. |
| 3694.0 | $2^{+}, 3^{\pm}, 4^{\pm}$ | Transitions to $4^{+}$ 2307-keV and $3^{-}$ 2880-keV levels, plus $\log ft = 8.2$. |
| 3922.6 | $(3^{-})$ | Possibly the neutron particle-hole state (Ref. 8) of $3^{-}$; consistent with transitions to $2^{+}$ 1435-keV, $4^{+}$ 1898-keV, and $3^{-}$ 2880-keV levels; $\log ft = 8.1$ indicates a hindered allowed $\beta$ branch. |
| 3935.2 | $2^{+}$ | Transition to ground state, plus $\log f_1 t = 8.5$. |
| 4012.3 | $3^{\pm}, 4^{+}, (2^{+})$ | Transition to $4^{+}$ 1898-keV level and 3643-keV level with maximum $J^{\pi}$ of $2^{+}$. Absence of ground-state transition favors $J = 3$ or 4. |
| 4080.1 | $(2^{-})$ | Possibly the neutron particle-hole state (Ref. 8) of $2^{-}$; consistent with the relatively strong $\gamma$ transition to the $3^{-}$ 2880-keV level. |
| 4242.4 | $2^{\pm}, 3^{\pm}, 4^{+}$ | Transition to $2^{+}$ 1435-keV level plus $\log f_1 t = 8.5$. |
| 4508.1 | $2^{+}, 3^{\pm}, 4^{+}$ | Transitions to $2^{+}$ 1435-keV and $4^{+}$ 1898-keV levels plus $\log f_1 t = 7.6$. |
| 4629.8 | $2^{+}, 3^{\pm}, 4^{\pm}$ | Transition to $4^{+}$ 1898-keV level plus $\log f_1 t = 7.0$. |

### C. Spin and parity assignments

The spin and parity assignments given on the level schemes are discussed in abbreviated form in Tables V and VI. The standards used for spin and parity assignments from $\log ft$ values are those adopted by the Nuclear Data Group.[35,36] The standards used for spin assignments based on strong $\gamma$-ray transitions are as follows:

If $\Delta\pi = +$, $\Delta J \leq 2$ since stronger $\gamma$-ray transitions are expected to be $M1$ or $E2$:

If $\Delta\pi = -$, $\Delta J \leq 1$ since stronger $\gamma$-ray transitions are expected to be $E1$.

In order for $M2$ transitions to compete with $E1$ transitions the latter must be hindered by a factor of greater than $10^{8}$, a situation not expected near a closed shell.

## IV. DISCUSSION

### A. Interpretation of the $^{138}$Cs levels

To discuss possible configurations for the various states in $^{138}$Cs, consider that the locations of the negative-parity neutron states, as determined by Fulmer, McCarthy, and Cohen,[12] are: $2f_{7/2}$, 0.0 MeV; $3p_{3/2}$, 0.83 MeV; $2f_{5/2}$, 1.88 MeV; $1h_{9/2}$, 1.9 MeV; and $3p_{1/2}$, 2.3 MeV. The positive-parity proton states and their energies, as calculated by Wildenthal,[26] are: $1g_{7/2}$, 0.0 MeV; $2d_{5/2}$, 0.52 MeV; $3s_{1/2}$, 2.95 MeV; and $2d_{3/2}$, 3.12 MeV. The only other single-particle states to consider without crossing the major shell closures are the positive-parity neutron state, $1i_{13/2}$, and the negative-parity proton state, $1h_{11/2}$.

From a simple single-particle picture of this nucleus, the negative-parity level structure below approximately 1.5 MeV would be made up of the configurations $\nu(f_{7/2})^1\pi(g_{7/2})^5$ ($E=0$, $J=0\rightarrow 7$), $\nu(f_{7/2})^1\pi(d_{5/2})^1\pi(g_{7/2})^4$ ($E=0.52$ MeV, $J=1\rightarrow 6$), $\nu(p_{3/2})^1\pi(g_{7/2})^5$ ($E=0.83$ MeV, $J=2\rightarrow 5$), $\nu(f_{7/2})^1\pi(d_{5/2})^2\pi(g_{7/2})^3$ ($E=1.04$ MeV, $J=0\rightarrow 7$), and $\nu(p_{3/2})^1\pi(d_{5/2})^1\pi(g_{7/2})^4$ ($E=1.35$ MeV, $J=1\rightarrow 4$). The principal two-particle interaction which removes the degeneracies in $J$ value and gives the low-energy negative-parity states is assumed to be the coupling of the odd neutron with the odd proton. The proton-proton interactions should be more energetic, as evidenced by the first-excited states in the $N = 82$ nuclei $^{136}$Xe and $^{138}$Ba which are regarded as pure proton-proton interactions. The neutron-proton coupled configurations can be expected to couple with the first proton-proton $2^+$ state at approximately 1.5 MeV to give further possible states. As the energy increases, the number of possible configurations grows and the interpretation of the levels becomes extremely difficult. For this reason configuration matching to states will be attempted only for the low-energy negative-parity states and the positive-parity states responsible for the allowed $\beta$ decays which have been observed.

The ground-state single-particle configuration, $\nu(f_{7/2})^1\pi(g_{7/2})^5$, is considered the dominant configuration for the states below 100 keV. The odd $2f_{7/2}$ neutron couples with the odd $1g_{7/2}$ proton to give a set of states with $J^\pi$ values between $0^-$ and $7^-$. Four of these states have probably been observed, the $3^-$, $2^-$, and $1^-$ states corresponding to the first three levels reported in this work, by Monnand *et al.*,[28] and by Achterberg *et al.*,[27] and the $6^-$ isomeric state at 79 keV reported by Carraz, Monnand, and Moussa.[17]

In the simple single-particle picture, there is not an abundance of low-spin $0^-$ and $1^-$ state available at low energies. Four states in the $^{138}$Cs level structure below 500 keV are candidates for these $J^\pi$ assignments. The 15.7-keV level has a $J^\pi$ assignment of $1^-$, the 258.3-keV level is $1^-$ or $2^-$, and the 412.1- and 450.2-keV levels are $0^-$ or $1^-$. The lack of $0^-$ and $1^-$ states available from the single-particle picture suggests that 2 is the proper spin assignment for the 258.3-keV level which makes it possible to explain the 412.1- and 450.2-keV levels in terms of the configurations with single-particle energies of 0.0 and 0.52 MeV.

Positive-parity states in the $^{138}$Cs nuclear structure can be formed by single-particle excitations of either a neutron into the positive-parity $1i_{13/2}$ state or a proton into the negative-parity $1h_{11/2}$ state. Other single-particle excitations involve crossing the large energy gaps responsible for the magic-number shell closures of 82 and 126. Positive-parity states could also be formed by exciting a core proton or neutron to form a particle-hole state. The latter possibility would result in excitations not observable in decay studies as evidenced by the neutron particle-hole states reported at about 3.5 MeV by Morrison *et al.*[8] in $^{138}$Ba which are above the $Q$ value of 2.83 MeV. Even if lower in energy, these states could not be populated by allowed $\beta$ transitions from $^{138}$Xe because transitions to these states are not possible with only single-particle processes. From the location of the $3^-$ octupole state in $^{138}$Ba, states formed by coupling negative-parity states to the octupole core excitation are expected to be above 2.8 MeV, also at the upper energy limit of states observable from the $\beta$ decay of $^{138}$Xe. Also, as noticed for the $^{138}$Cs decay, the $\beta$ branching to the $3^-$ octupole state in $^{138}$Ba is a hindered transition. From these considerations, positive-parity states receiving allowed $\beta$ transitions are most reasonably explained by single-particle excitations.

The lowest-energy positive-parity states in $^{138}$Cs would involve the configurations $\nu(i_{13/2})^1\pi(g_{7/2})^5$ or $\nu(f_{7/2})^1\pi(h_{11/2})^1\pi(g_{7/2})^4$. Other positive-parity states could be built on these states by either exciting the $2f_{7/2}$ neutron to another negative-parity state or a $1g_{7/2}$ proton to another positive-parity state. It should be noted that the simplest coupling schemes for these states give a minimum spin of 2 since the coupling involves a $2f_{7/2}$ neutron and $1h_{11/2}$ proton or an $1i_{13/2}$ neutron and $1g_{7/2}$ proton. Positive-parity states with spin of 1 are observed, however, indicating that either the paired protons are not coupling to zero, or a $2f_{7/2}$ neutron or $1g_{7/2}$ proton is being excited to a similar parity state with a higher $j$ value. The only single-particle excitation available without crossing a major shell boundary and satisfying the above conditions is $\nu(f_{7/2})\rightarrow\nu(h_{9/2})$, to give the configuration $\nu(h_{9/2})^1\pi(h_{11/2})^1\pi(g_{7/2})^4$.

The most likely configurations for the states to which allowed $\beta$ decay proceeds are then $\nu(i_{13/2})^1\pi(g_{7/2})^5$ or $\nu(f_{7/2})^1\pi(h_{11/2})^1\pi(g_{7/2})^4$ with the $1g_{7/2}$ protons not coupled to a spin of 0, or $\nu(h_{9/2})^1\pi(h_{11/2})^1\pi(g_{7/2})^4$ with the $1g_{7/2}$ protons coupling to a spin of 0. Since the single-particle excitation $\nu(f_{7/2})\rightarrow\nu(h_{9/2})$ involves about 1.9 MeV which is close to the proton-proton coupled $2^+$ level, both possibilities need to be considered.

Configuration mixing in the $^{138}$Xe ground state is required to reach these states since the dominant $^{138}$Xe ground-state configuration $\nu(f_{7/2})^2\,\pi(g_{7/2})^4$ cannot be connected to the above states by an allowed $\beta$ transition. Two configurations, $\nu(f_{7/2})^1\,\nu(h_{9/2})^1\,\pi(g_{7/2})^4$ and $\nu(h_{9/2})^2\,\pi(g_{7/2})^4$, which might be reasonably mixed in the ground state of $^{138}$Xe, could give rise to allowed $\beta$ decay to the states $\nu(f_{7/2})^1\,\pi(h_{11/2})^1\,\pi(g_{7/2})^4$ and $\nu(h_{9/2})^1\,\pi(h_{11/2})^1\,\pi(g_{7/2})^4$, respectively. From a theoretical viewpoint, the calculation of transition probabilities would be interesting. Only a few configurations contribute to the allowed $\beta$ decay, hopefully making the calculation possible.

### B. Interpretation of the $^{138}$Ba levels

Although a very complete shell-model calculation has been done by Wildenthal,[26] the results of a limited-basis shell-model calculation are briefly presented here to illustrate to what extent such a simple calculation can fit the actual data. Most experimental measurements[13, 14] indicate that the majority of the states in the lower half of the level structure of $^{138}$Ba consist of configurations involving protons in the $1g_{7/2}$ and $2d_{5/2}$ states; thus, only these two single-particle states were included in the calculation. One further simplification was made; four of the six orbital protons were frozen along with the core leaving only configurations with the remaining two protons to be considered. With these simplifications the shell-model calculation involves only three configurations. Using the single-particle energies of 0 MeV for the $1g_{7/2}$ shell and 0.52 MeV for the $2d_{5/2}$ shell determined in the calculation by Wildenthal,[26] single-particle energies for the three configurations would be 0, 0.52, and 1.04 MeV. The degeneracy in these single-particle energy states was removed by using a surface-$\delta$-interaction in which the radial wave functions were set equal at the nuclear surface. The level scheme shown in Fig. 4 results from using a $\delta$-interaction strength which gives a 1.435-MeV separation between the ground state and first excited state. For comparison, the experimental scheme of this work and the results of the calculation by Larson, Austin, and Wildenthal[37] are also shown in Fig. 4, up to the energy limits of the simplified calculation.

The calculation clearly has severe limitations since the $2d_{3/2}$ and $3s_{1/2}$ proton orbitals, as well as the configurations formed by freeing the four

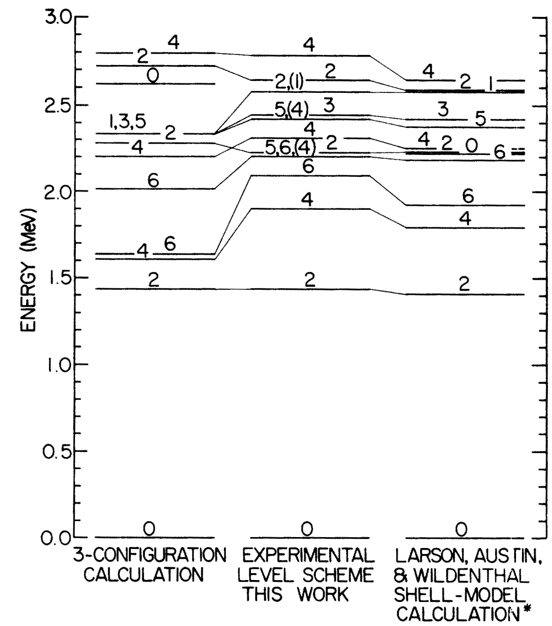


FIG. 4. Comparison of levels of $^{138}$Ba from restricted configuration shell-model calculation with results of this work and the calculation of Larson, Austin, and Wildenthal (Ref. 37).

frozen $1f_{7/2}$ protons, are not included. Measurements of the admixtures present in the $^{138}$Ba ground state by Wildenthal, Newman, and Auble[13] indicate that even paired $1h_{11/2}$ protons cannot be neglected entirely for an accurate description of the positive-parity states. Admitting these shortcomings, the calculation presented here illustrates how well a simple calculation can fit the actual data, although it is not intended to replace the more complete shell-model calculations.


### V. ACKNOWLEDGMENTS

It is a pleasure to acknowledge Dr. W. C. Schick, Jr., and Dr. F. K. Wohn, who developed most of the computer codes used in this study and also worked hard at perfecting the $\gamma$-ray and $\beta$-ray detection systems. Gratitude is also extended to Dr. B. S. Cooper for enlightening discussions which led to several of the ideas presented in the Discussion. The authors would also like to thank the members of the TRISTAN project who shared in its development and aided in the collection of the data presented in this work.

[1]B. L. Cohen and R. E. Price, Phys. Rev. 123, 283 (1961).
[2]O. Hansen and O. Nathan, Nucl. Phys. 42, 197 (1963).
[3]S. A. A. Zaidi, P. von Brentano, D. Rieck, and J. P. Wurm, Phys. Lett. 19, 45 (1965).
[4]J. Alster, E. J. Martens, and N. M. Alpert, Bull. Am. Phys. Soc. 13, 70 (1968).
[5]P. R. Christensen and F. C. Yang, Nucl. Phys. 72, 657 (1965).
[6]J. H. Barker and J. C. Hiebert, Phys. Rev. C 6, 1795 (1972).
[7]D. Larson, S. M. Austin, B. H. Wildenthal, and S. H. Fox, Bull. Am. Phys. Soc. 17, 52 (1972).
[8]G. C. Morrison, N. Williams, J. A. Nolen, and D. von Ehrenstein, Phys. Rev. Lett. 19, 592 (1967).
[9]D. S. Andreev, V. D. Vasil'ev, G. M. Gusinskii, K. I. Erokhina, and I. K. Lemberg, Izv. Akad. Nauk SSSR Ser. Fiz. 25, 861 (1961) [transl.: Bull. Acad. Sci. USSR Phys. Ser. 25, 842 (1961)].
[10]D. G. Alkhazov, D. S. Andreev, V. D. Vasil'ev. Yu. P. Gangrskii, I. K. Lemberg, and Yu. I. Udralov, Izv. Akad. Nauk SSSR Ser. Fiz. 27, 1285 (1963) [transl.: Bull. Acad. Sci. USSR Phys. Ser. 27, 1263 (1963)].
[11]R. A. Sorensen, E. K. Lin, and B. L. Cohen, Phys. Rev. 142, 729 (1966).
[12]R. H. Fulmer, A. L. McCarthy, and B. L. Cohen, Phys. Rev. 128, 1302 (1962).
[13]B. H. Wildenthal, E. Newman, and R. L. Auble, Phys. Rev. C 3, 1199 (1971).
[14]W. P. Jones, L. W. Borgman, K. T. Hecht, J. Bardwick, and W. C. Parkinson, Phys. Rev. C 4, 580 (1971).
[15]M. A. J. Mariscotti, W. Gelletly, J. A. Moragues, and W. R. Kane, Phys. Rev. 174, 1485 (1968).
[16]L. V. Groshev, V. N. Dvoretskii, A. M. Demidov, and A. S. Rakhimov, Izv. Akad. Nauk SSSR Ser. Fiz. 34, 768 (1970) [transl.: Bull. Acad. Sci. USSR Phys. Ser. 34, 680 (1970)].
[17]L. C. Carraz, E. Monnand, and A. Moussa, Nucl. Phys. A171, 209 (1971).
[18]L. M. Langer, R. B. Duffield, and C. W. Stanley, Phys. Rev. 89, 907 (1953).
[19]M. E. Bunker, R. B. Duffield, J. Mize, and J. W. Starner, Phys. Rev. 103, 1417 (1956).
[20]W. M. Currie, Nucl. Phys. 48, 561 (1963).
[21]G. H. Carlson, W. C. Schick, Jr., W. L. Talbert, Jr., and F. K. Wohn, Nucl. Phys. A125, 267 (1969).
[22]T. Alväger, R. A. Naumann, R. F. Petry, G. Sidenius, and T. D. Thomas, Phys. Rev. 167, 1105 (1968).
[23]T. Nagahara, N. Miyaii, H. Kurihara, Y. Mizuno, and Y. Ishizuka, J. Phys. Soc. Jap. 28, 283 (1970).
[24]J. C. Hill and D. F. Fuller, Phys. Rev. C 5, 532 (1972).
[25]E. Achterberg, F. C. Iglesias, A. E. Jech, J. A. Moragues, D. Otero, M. L. Pérez, A. N. Proto, J. J. Rossi, W. Scheuer, and J. F. Suárez, Phys. Rev. C 5, 1759 (1972).
[26]B. H. Wildenthal, Phys. Rev. Lett. 22, 1118 (1969).
[27]E. Achterberg, F. C. Iglesias, A. E. Jech, J. A. Moragues, D. Otero, M. L. Pérez, A. N. Proto, J. J. Rossi, W. Scheuer, and J. F. Suárez, Phys. Rev. C 7, 365 (1973).
[28]E. Monnand, R. Brissot, L. C. Carraz, J. Crancon, C. Ristori, F. Schussler, and A. Moussa, Nucl. Phys. A195, 192 (1972).
[29]W. L. Talbert, Jr., and D. Thomas, Nucl. Instrum. Methods 38, 306 (1965).
[30]W. L. Talbert, Jr., and J. R. McConnell, Ark. Fys. 36, 99 (1967).
[31]G. H. Carlson, Ph.D. thesis, Iowa State University, 1972 (unpublished).
[32]F. K. Wohn. J. R. Cifford, G. H. Carlson, and W. L. Talbert, Jr., Nucl. Instrum. Methods 101, 343 (1972).
[33]J. P. Adams, W. L. Talbert, Jr., F. K. Wohn, G. H. Carlson, J. R. Clifford, M. A. Lee, and J. R. McConnell, Phys. Rev. C 8, 767 (1973).
[34]G. M. Stinson, N. P. Archer, J. C. Waddington, and R. G. Summers-Gill, Can. J. Phys. 45, 3393 (1967).
[35]S. Raman and N. B. Gove, Phys. Rev. C 7, 1995 (1973).
[36]N. B. Gove and M. J. Martin, Nucl. Data A10, 205 (1971).
[37]D. Larson, S. M. Austin, and B. H. Wildenthal, Phys. Lett. 42B, 153 (1972); and private communication.